

ARTICULATED WHEELED ROBOTS: EXPLOITING RECONFIGURABILITY AND REDUNDANCY

Qiushi Fu

Mechanical and Aerospace Engineering
State University of New York at Buffalo
Buffalo, New York, 14260
qiushifu@buffalo.edu

Venkat Krovi

Mechanical and Aerospace Engineering
State University of New York at Buffalo
Buffalo, New York, 14260
vkrovi@eng.buffalo.edu

ABSTRACT

Articulated Wheeled Robotic (AWR) locomotion systems consist of chassis connected to a set of wheels through articulated linkages. Such articulated “leg-wheel systems” facilitate reconfigurability that has significant applications in many arenas, but also engender constraints that make the design, analysis and control difficult. We will study this class of systems in the context of design, analysis and control of a novel planar reconfigurable omnidirectional wheeled mobile platform. We first extend a twist based modeling approach to this class of AWRs. Our systematic symbolic implementation allows for rapid formulation of kinematic models for the general class of AWR. Two kinematic control schemes are developed which coordinate the motion of the articulated legs and wheels and resolve redundancy. Simulation results are presented to validate the control algorithm that can move the robot from one configuration to another while following a reference path. The development of two generations of prototypes is also presented briefly.

INTRODUCTION

In recent times, a new class of robotic locomotion systems – articulated wheeled robot (AWR) – consisting of a main chassis connected to a set of wheels with ground contact via articulated chains have been proposed. This class of so called ‘leg-wheeled’ systems has been getting considerable attentions due to their advantages over traditional wheeled systems and legged systems in various applications as planetary explorations [1, 2], agriculture [3], rescue operations and wheelchairs [4]. Adding articulations between the wheels and chassis allows the wheel placement with respect to chassis to change during locomotion either passively or actively, thus AWRs can be briefly divided into these two categories.

The main research in passive AWRs concerns designing suspension mechanism to negotiate with the uneven terrain. The planetary rovers [1] developed at Jet Propulsion Laboratory (JPL) and the Shrimp rover [2] have shown enhanced terrain adaptability featuring novel suspension design such as rocker-bogie and four-

bar mechanism. They change their configuration according to the changing terrain topology. Passive AWRs are usually designed to have fewer degrees of freedom (DOFs) such that the weight of the system can be supported by the structure. The main advantages of passive AWRs are in terms of power consumption, payload capacity, and controller design.

Active articulations further enhance the mobility of the robots to obtain better performance, such as stability and traction. They have been demonstrated by sample return rover (SRR) [5], ATHLETE rover [6], WAAV [7], Workpartner [3], Hylos [8], and variable footprint wheel chair [4]. The redundant actuated DOFs bring the system capability to optimize certain performance index such as stability. On the other hand, more actuators add extra weight and control complexity.

In most applications, the wheel of AWRs is considered as a rigid disk with a single point of contact with the terrain surface. This means that the motion of the wheel is restricted by nonholonomic constraints. These constraints could be violated with slipping and skidding which are main sources of large energy consumption and measurement uncertainty. Minimization of slipping and skidding is usually desired and can be achieved either by a good kinematic design or proper cooperation of the rolling or steering of the wheels. Holonomic constraints in the articulations also increase the complexity of the system for people to relate the motion between wheels and chassis. Thus, the design, navigation and control of AWRs require a general framework for systematic kinematic modeling and analysis. Kinematic modeling of ordinary wheeled robots (OWRs, which can be seen as a subset of AWRs) has been dealt extensively. Muir and Newman [9] derived the equation of motion of OWRs using matrix transformation. Campion *et al.* [10] classified OWRs based on kinematic models developed using vector approach and nonholonomic constraints. Yi and Kim [11] presented modeling of omnidirectional wheeled robots with slipping. Fewer efforts have been focusing on AWRs. Grand *et al.* [8] presented a general geometric modeling approach and controlled the locomotion and posture separately. Tarokh and McDermott [12] used symbolic derivatives of transformation

matrices with consideration of wheel slip and discussed three different kinematic forms for passive rovers. Choi and Sreenivasan [13] construct the kinematic model using screws and proposed a force distribution algorithm.

Twist based approaches have been used to analyze motion and force capabilities systematically in other contexts, such as for parallel manipulators or multifinger grasping. However such methods have not been reported for modeling of AWRs, and especially articulated systems with rolling wheel ground contacts. Thus, one of the principal contributions of this paper is to extend the systematic twist-based modeling framework to this class of AWRs. Further, automating this process by using the symbolic toolbox in MATLAB, facilitates the rapid modeling and analysis of any given design of an AWR.

We will also illustrate our modeling process in the context of design and analysis of a novel articulated omnidirectional robot – the ROAMeR. Traditional planar wheeled platforms in indoor application driven by fixed or centered orientable wheels are subjected to nonholonomic constraints which restricts the motion of the overall system [10]. In practice, such vehicles are typically unable to move their payload in all directions with equal ease. Hence there has been an increased interest in developing wheeled platform with omnidirectional motion capability. Many omnidirectional vehicle designs have been proposed using Mecanum/Swedish or Ball wheels. Wada and Asada [4] built a reconfigurable wheelchair using ball wheels. Song and Byun [14] presented a robot with steerable omni-directional wheels. Such systems face many challenges including discontinuous ground contact, poor ground clearance, or complicated mechanical design. Hence an exclusively disk-wheeled based design is preferred from the view point of ease of actuation and robustness. However, additional articulations need to be introduced in order to allow for adequate mobility within the system. Caster wheels have been implemented as the simplest articulated wheel for allowing omnidirectional mobility. For example, Yi and Kim [11] and Holmberg and Khatib [15] built and analyzed omnidirectional robots driven by powered caster wheels – however, the locations of the caster wheel w.r.t the chassis are always constant.

The presence of more articulations within the leg-wheel chain further provides reconfigurability by allowing relocation of the wheel with respect to the chassis. There are many scenarios where planar AWRs could benefit from reconfigurability (which in the past has often only been explored in the context of uneven terrain locomotion). For instance, the robot base may need to be compact when passing a narrow doorway and be extended to enhance stability when manipulating heavy objects. Hence in this paper we examine a wheeled platform design (with active articulations and actively driven disk wheels) for the purpose of achieving omnidirectional mobility together with the ability to reconfigure for different tasks. The modeling and control complexity of the ROAMeR increase with the addition of these articulations and their interaction with the contact constraints. We will address the modeling within the twist based framework leading up to development of 2 kinematic control laws for our ROAMeR. The

focus of these laws is on resolving the redundancy while allowing for simultaneous trajectory tracking and configuration control of the ROAMeR.

The rest of the paper is organized as follows: Section 2 discusses twist based modeling. Modeling of a planar reconfigurable omnidirectional robot is presented in Section 3. In Section 4, two kinematic control schemes are proposed. Section 5 discusses the simulation result, followed by prototypes in Section 6. Section 7 concludes the paper.

TWIST BASED KINEMATIC MODELING

As we are focusing on AWRs, we will not discuss the cases where the robot has contact points to the ground that is not on the wheel. To establish the kinematic model that relates the motion of the robot body and the motion of the wheels and linkages, we will first define frames of reference properly, then find the twists expressed in a sequence of local frames starting from body fixed frame. By appropriate transformation, we can express any twist in one single frame and assemble them as the Jacobian matrix of the robot.

A general model of AWR is shown in Fig. 1, we define an inertial frame of reference $\{F\} = (O_f, \vec{X}, \vec{Y}, \vec{Z})$, and at any time, the robot has an instantaneous frame $\{B\} = (O_b, \vec{b}_x, \vec{b}_y, \vec{b}_z)$ attached to its body that moves with the robot, where O_b is the point of interest on the robot (Center of Mass is often chosen). The configuration of the main body could be defined as $[x \ y \ z \ \phi \ \theta \ \psi]^T$ with respect to the inertial frame.

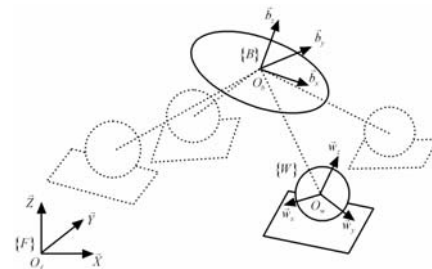


FIGURE 1: GENERAL ARTICULATED WHEEL ROBOT

The robot could possess n branches. Each of them consists of any number of linkages and end with one wheel. Each wheel has a coordinate frame $\{W\} = (O_w, \vec{w}_x, \vec{w}_y, \vec{w}_z)$ attached to the wheel axle (for simplicity, we will neglect the subscript i for labeling branch), O_w is the center of the wheel and \vec{w}_z lies on the wheel axle. The dashed line in the figure between the chassis and the wheel represents any set of links and joints that exists between these two frames, including the steering and suspension mechanism. We define ${}^B A_{A_0}$ the transformation between body frame and joint 1 frame, ${}^{j-1} A_j, j = 1, 2, \dots, m-1$ the transformation between joint j and joint $j+1$ frame, ${}^m A_w$ the transformation between joint m frame and wheel frame. These transformations can be expressed easily using D-H parameters.

In our model, each wheel is assumed to be represented by a rigid disc with a single point of contact with the terrain surface. The wheel plane is defined at the center of the wheel and perpendicular to the wheel axle (\bar{w}_z), that is, the plane formed by \bar{w}_x and \bar{w}_y . and a tangent contact plane is defined perpendicular to the wheel plane at the contact point, as shown in Fig. 2.

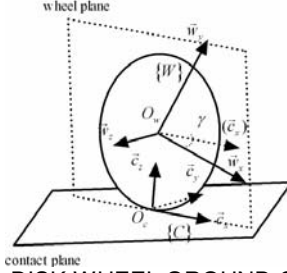


FIGURE 2: RIGID DISK WHEEL GROUND CONTACT MODEL

Multiple contact points on wheel offer a challenge for analysis and control and we will not consider it for the present. In the real application it is also quite difficult to sense or estimate the position of multiple contact points. For the single point contact, a contact frame $\{C\} = (O_c, \bar{c}_x, \bar{c}_y, \bar{c}_z)$ is defined as the contact frame assigned at each wheel's contact point as illustrated in Fig. 2, where \bar{c}_z is a unit vector in the wheel plane and normal to the tangent contact plane at the point of contact, that is, a vector point to the center of the wheel. $\bar{c}_x = \bar{c}_z \times \bar{w}_z$, and $\bar{c}_y = \bar{c}_z \times \bar{c}_x$. γ is the contact angle defined as the angle between \bar{c}_x and \bar{w}_x , since \bar{c}_x is always lies in the wheel plane. This angle varies when the AWR is moving on uneven terrain or performing reconfiguration. It can be measured using force sensor on the wheel axle (or estimated). The transformation between the wheel frame and contact frame is denoted by the homogeneous transformation

$${}^w A_C = \begin{bmatrix} \cos \gamma & 0 & -\sin \gamma & r \sin \gamma \\ \sin \gamma & 0 & \cos \gamma & -r \cos \gamma \\ 0 & -1 & 0 & 0 \\ 0 & 0 & 0 & 1 \end{bmatrix} \quad (1)$$

The homogeneous transformation between any two frames can be obtained by matrix multiplication and inversion. For instance, ${}^B A_W$ can be written as successive multiplication of several homogeneous transformations

$${}^B A_W = {}^B A_{A_0} {}^{A_0} A_{A_1} \cdots {}^{A_m} A_W \quad (2)$$

and overall transformation from body frame to contact frame can be found as

$${}^B A_C = {}^B A_W {}^W A_C \quad (3)$$

We define the velocity of the main body with respect to inertial frame expressed in body frame as ${}^B [{}^F V_B]$. The velocity of contact frame with respect to inertial frame expressed in contact frame is defined as ${}^C [{}^F V_C]$. In order to find the 6 dimensional twist vector representing joint velocity in local frame ${}^b [{}^a V_b]$, one can either write it out directly (it is usually a simple motion for a

single joint) or compute it by first finding the twist matrix and extract out the twist vector. The twist matrix is given by

$${}^b [{}^a T_b] = {}^a A_b^{-1} \cdot {}^a A_b^T = \begin{bmatrix} \Omega_{3 \times 3} & v_{3 \times 1} \\ 0 & 0 \end{bmatrix} \quad (4)$$

where ${}^a A_b$ is the homogeneous transformation between two frames a and b , $v_{3 \times 1} = [v_1 \ v_2 \ v_3]^T$ is the translational velocity and Ω is a 3×3 skew symmetric matrix that represents the angular velocity of frame b with respect to frame a expressed in b

$$\Omega_{3 \times 3} = \begin{bmatrix} 0 & -\omega_3 & \omega_2 \\ \omega_3 & 0 & -\omega_1 \\ -\omega_2 & \omega_1 & 0 \end{bmatrix} \quad (5)$$

Then the twist vector can be found by

$${}^b [{}^a V_b] = {}^b [{}^a T_b]^\vee = [v_1 \ v_2 \ v_3 \ \omega_1 \ \omega_2 \ \omega_3]^T \quad (6)$$

where \vee is an operator that extract out the velocity vector.

The velocity of contact frame can be obtained by summing body twist and all joint twists in the contact frame

$$\begin{aligned} {}^C [{}^F V_C] &= {}^C Ad_B \cdot {}^B [{}^F V_B] + {}^C Ad_{A_1} \cdot {}^{A_1} [{}^B V_{A_1}] \\ &+ {}^C Ad_{A_2} \cdot {}^{A_2} [{}^{A_1} V_{A_2}] + \cdots + {}^C Ad_{A_m} \cdot {}^{A_m} [{}^{A_{m-1}} V_{A_m}] \\ &+ {}^C Ad_W \cdot {}^W [{}^F V_W] + {}^C [{}^W V_C] \end{aligned} \quad (7)$$

where ${}^a Ad_b$ is the adjoint transformation matrix that transform twist vectors from frame b to frame a

$${}^a Ad_b = \begin{bmatrix} {}^a R_b & \hat{p}_b {}^a R_b \\ 0 & {}^a R_b \end{bmatrix} \quad (8)$$

where ${}^a R_b$ and \hat{p}_b are the rotational and translational parts of homogenous transformation ${}^a A_b$. Since joint twists can be written as the product of direction and magnitude as

$$[{}^c Ad_b]_{6 \times 6} \cdot {}^b [{}^a V_b]_{6 \times 1} = [{}^a t_b]_{6 \times 1} \dot{\theta} \quad (9)$$

we can rewrite the equation as

$${}^C [{}^F V_C] = {}^C Ad_B \cdot {}^B [{}^F V_B] + B \dot{q} \quad (10)$$

where $B = [{}^C [{}^{A_1} t_{A_2}] \ \cdots \ {}^C [{}^{A_{m-1}} t_{A_m}] \ {}^C [{}^{A_m} t_W] \ {}^C [{}^W t_C]]$ is a twist assembled matrix and $\dot{q} = [\dot{\theta}_1 \ \cdots \ \dot{\theta}_{m-1} \ \dot{\theta}_m \ \dot{\phi}]^T$ is a vector consists of m joint variables through the chain and the wheel rotational velocity $\dot{\phi}$. The pure rolling contact condition at the contact point which can be represented as

$$S^T {}^C [{}^F V_C] = [0 \ 0 \ 0]^T \quad \text{where } S^T = [I_{3 \times 3} \ 0_{3 \times 3}] \quad (11)$$

where S is a wrench basis matrix that represents the direction where force can be exerted. It actually selects the first three rows of the twist vector and restricts the translational motion at the contact point. For one branch of an AWR, if pure rolling condition is assumed, we can rewrite the Eq. (11) as

$$-S^T {}^C Ad_B \cdot {}^B [{}^F V_B] = S^T B \dot{q} \quad \text{and } M {}^B [{}^F V_B] = J \dot{q} \quad (12)$$

For all branches of the AWR, we can assemble equations as:

$$\begin{bmatrix} M_1 \\ M_2 \\ \vdots \\ M_n \end{bmatrix} {}^B [{}^F V_B] = \begin{bmatrix} J_1 & 0 & 0 & 0 \\ 0 & J_2 & 0 & 0 \\ 0 & 0 & \ddots & 0 \\ 0 & 0 & 0 & J_n \end{bmatrix} \begin{bmatrix} \dot{q}_1 \\ \dot{q}_2 \\ \vdots \\ \dot{q}_n \end{bmatrix} \quad (13)$$

Thus the twist based modeling approach offers a systematic framework for symbolic formulation of governing equations.

EXAMPLE: A RECONFIGURABLE OMNIDIRECTIONAL PLANAR MOBILE ROBOT

In this section, we will present a new design of mobile robot that can change its configuration while moving on the floor omnidirectionally, Reconfigurable Omnidirectional Articulated Mobile Robot (ROAMeR). The ROAMeR is a planar AWR where most of the issues of general AWRs exist, such as multiple constraints and redundancy, though the wheel ground contact angle will not be considered since it is a constant zero. Constraints at contact points restrict the motion of the components of the system such that the cooperation of the actuators is not straight forward and redundancy in the system further complicates the control. One can systematically deal with the overall effect of all constraints on the motion by using our twist based modeling approach, then a controller could be designed by putting the kinematic model into different forms. In this paper, the ROAMeR will be our first step to investigate AWRs with our modeling framework.

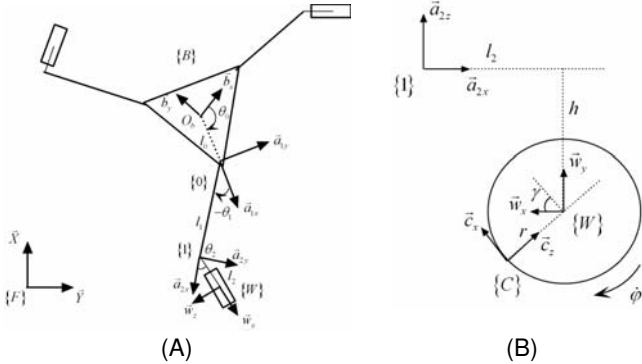


FIGURE 3: KINEMATIC MODELING OF RECONFIGURABLE OMNIDIRECTIONAL ROBOT: (A) FRAME OF REFERENCES AT THE JOINTS AND (B) CONTACT FRAME

The ROAMeR has a main body that is connected to three links (legs) by revolute joints, the three branches end with caster wheels. The arrangement of the wheels can be changed by varying the angle of the joint that connect the links and chassis (posture joints). The vehicle remains omnidirectional with the caster wheels. To establish the kinematic model of this design, we will follow the procedure proposed in the previous section, we first assign frames as shown in Fig. 3, as we are using a symmetric design, we will only show the derivation for one branch. The body attached frame $\{B\} = (O_b, \vec{b}_x, \vec{b}_y, \vec{b}_z)$ is put at the center of mass of the main body. Frame $\{A_0\}$ is located at the first revolute joint of the articulation, $\{A_1\}$ at the second revolute joint (caster wheel steering), $\{W\}$ at the axle of the wheel (caster wheel driving),

$\{C\}$ at the contact point. The D-H parameters are shown in Table.1.

TABLE 1: D-H PARAMETERS OF THE ROAMER

Joint	α	a	d	θ
1 posture $\{A_0\}$	0	l_0	0	θ_0
2 steering $\{A_1\}$	0	l_1	0	θ_1
3 driving $\{W\}$	$\pi/2$	l_2	$-h$	θ_2

With D-H parameters, it is easy to obtain the homogeneous transformation matrices between adjoint frames.

$${}^B A_{A_0} = \begin{bmatrix} c_0 & -s_0 & 0 & l_0 c_0 \\ s_0 & c_0 & 0 & l_0 s_0 \\ 0 & 0 & 1 & 0 \\ 0 & 0 & 0 & 1 \end{bmatrix}, {}^{A_0} A_{A_1} = \begin{bmatrix} c_1 & -s_1 & 0 & l_1 c_1 \\ s_1 & c_1 & 0 & l_1 s_1 \\ 0 & 0 & 1 & 0 \\ 0 & 0 & 0 & 1 \end{bmatrix}$$

$${}^{A_1} A_W = \begin{bmatrix} c_2 & 0 & s_2 & l_2 c_2 \\ s_2 & 0 & -c_2 & l_2 s_2 \\ 0 & 1 & 0 & -h \\ 0 & 0 & 0 & 1 \end{bmatrix}, {}^W A_C = \begin{bmatrix} c_\gamma & 0 & -s_\gamma & r s_\gamma \\ s_\gamma & 0 & c_\gamma & -r c_\gamma \\ 0 & -1 & 0 & 0 \\ 0 & 0 & 0 & 1 \end{bmatrix}$$

Twist vectors expressed in local frames are found as

$${}^B [{}^F V_B] = [\dot{x} \quad \dot{y} \quad \dot{z} \quad \dot{\phi} \quad \dot{\theta} \quad \dot{\psi}]^T$$

$${}^{A_0} [{}^B V_{A_0}] = 0$$

$${}^{A_1} [{}^{A_0} V_{A_1}] = [0 \quad l_1 \dot{\theta}_1 \quad 0 \quad 0 \quad 0 \quad \dot{\theta}_1]^T$$

$${}^W [{}^{A_1} V_W] = [0 \quad 0 \quad 0 \quad 0 \quad -\dot{\theta}_2 \quad 0]^T$$

$${}^C [{}^W V_C] = [r \dot{\phi} \quad 0 \quad 0 \quad 0 \quad -\dot{\phi} \quad 0]^T$$

Contact twist expressed in contact frame is

$${}^C [{}^r V_C] = {}^C Ad_B \cdot {}^B [{}^F V_B] + {}^C Ad_{A_0} \cdot {}^{A_0} [{}^B V_{A_0}] + {}^C Ad_{A_1} \cdot {}^{A_1} [{}^{A_0} V_{A_1}] + {}^C Ad_W \cdot {}^W [{}^{A_1} V_W] + {}^C [{}^W V_C] \quad (14)$$

Apply the nonholonomic constraint to the system using Eq. (13), we could get

$$M {}^B [{}^F V_B] = J \dot{q} \quad (15)$$

As the ROAMeR is moving on a flat terrain, only planar motion in xy plane are considered, we can further simplify the constraints for each chain to:

$$\begin{bmatrix} c_{012} & s_{012} & l_0 s_{12} + l_1 s_2 \\ -s_{012} & c_{012} & l_0 c_{12} + l_1 c_2 + l_2 \end{bmatrix} \dot{X}_b = \begin{bmatrix} -r & -l_1 s_2 & 0 \\ 0 & -l_1 c_2 - l_2 & -l_2 \end{bmatrix} \begin{bmatrix} \dot{\phi} \\ \dot{\theta}_1 \\ \dot{\theta}_2 \end{bmatrix}$$

where $\dot{X}_b = [\dot{x}_b \quad \dot{y}_b \quad \dot{\psi}_b]^T$ is the chassis velocity in horizontal plane with respect to body frame. We can then assemble the overall kinematic equation from all three branches as

$$P_A \dot{X}_b = Q_A \dot{q}_A \quad (16)$$

where $\dot{q}_A = [\dot{\varphi}_1 \ \dot{\theta}_{12} \ \dot{\theta}_{11} \ \dot{\varphi}_2 \ \dot{\theta}_{22} \ \dot{\theta}_{21} \ \dot{\varphi}_3 \ \dot{\theta}_{32} \ \dot{\theta}_{31}]^T$

$$P_A = \begin{bmatrix} c_{012}^1 & s_{012}^1 & l_0 s_{12}^1 + l_1 s_2^1 \\ -s_{012}^1 & c_{012}^1 & l_0 c_{12}^1 + l_1 c_2^1 + l_2 \\ c_{012}^2 & s_{012}^2 & l_0 s_{12}^2 + l_1 s_2^2 \\ -s_{012}^2 & c_{012}^2 & l_0 c_{12}^2 + l_1 c_2^2 + l_2 \\ c_{012}^3 & s_{012}^3 & l_0 s_{12}^3 + l_1 s_2^3 \\ -s_{012}^3 & c_{012}^3 & l_0 c_{12}^3 + l_1 c_2^3 + l_2 \end{bmatrix}$$

$$Q_A = \begin{bmatrix} r & 0 & l_1 s_2^1 & 0 & 0 & 0 & 0 & 0 & 0 \\ 0 & l_2 & l_1 c_2^1 + l_2 & 0 & 0 & 0 & 0 & 0 & 0 \\ 0 & 0 & 0 & r & 0 & l_1 s_2^2 & 0 & 0 & 0 \\ 0 & 0 & 0 & 0 & l_2 & l_1 c_2^2 + l_2 & 0 & 0 & 0 \\ 0 & 0 & 0 & 0 & 0 & 0 & r & 0 & l_1 s_2^3 \\ 0 & 0 & 0 & 0 & 0 & 0 & 0 & l_2 & l_1 c_2^3 + l_2 \end{bmatrix}$$

KINEMATIC CONTROL OF THE ROAMER

We have formed the kinematic equations of the ROAMeR in the previous section. The purpose of this planar AWR design is to enable the robot to change the arrangement of its legs while moving around. Thus there are two control tasks, the first one is path following in Cartesian space (x, y, ψ) , the second one is position regulation in sub joint space $(\theta_{11}, \theta_{21}, \theta_{31})$. The robot has totally 9 joints available to be actuated but the task is only 6 dimensional. The robot possesses both kinematic redundancy and actuation redundancy that needs to be resolved. We will be focusing on kinematic redundancy in this paper. The basic control law we will use is close loop resolved motion rate control (RMRC), in which we map the desire task space velocity into joint space and each joint velocity will be controlled independently using simple PI controller. Error space control law is used to close the control loop.

Control Scheme I

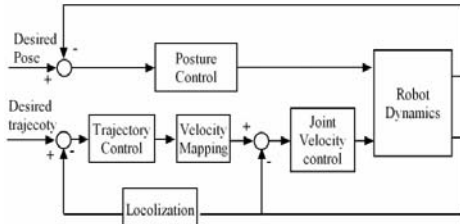


FIGURE 4: DIAGRAM OF KINEMATIC CONTROL SCHEME I

In the first control scheme, we determine the speed of hip joints explicitly. Once the desired hip joint velocities are determined, it can be used to assist finding the velocities of other joints. We modify the forward kinematic equation obtained in the previous section into a more convenient form

$$P_C \dot{X} = Q_C \dot{q}_C \quad (17)$$

where

$$\dot{X} = [\dot{x}_b \ \dot{y}_b \ \dot{\psi}_b \ \dot{\theta}_{11} \ \dot{\theta}_{21} \ \dot{\theta}_{31}]^T$$

$$\dot{q}_C = [\dot{\varphi}_1 \ \dot{\theta}_{12} \ \dot{\varphi}_2 \ \dot{\theta}_{22} \ \dot{\varphi}_3 \ \dot{\theta}_{32}]^T$$

$$P_C = \begin{bmatrix} c_{012}^1 & s_{012}^1 & l_0 s_{12}^1 + l_1 s_2^1 & l_1 s_2^1 & 0 & 0 \\ -s_{012}^1 & c_{012}^1 & l_0 c_{12}^1 + l_1 c_2^1 + l_2 & l_1 c_2^1 + l_2 & 0 & 0 \\ c_{012}^2 & s_{012}^2 & l_0 s_{12}^2 + l_1 s_2^2 & 0 & l_1 s_2^2 & 0 \\ -s_{012}^2 & c_{012}^2 & l_0 c_{12}^2 + l_1 c_2^2 + l_2 & 0 & l_1 c_2^2 + l_2 & 0 \\ c_{012}^3 & s_{012}^3 & l_0 s_{12}^3 + l_1 s_2^3 & 0 & 0 & l_1 s_2^3 \\ -s_{012}^3 & c_{012}^3 & l_0 c_{12}^3 + l_1 c_2^3 + l_2 & 0 & 0 & l_1 c_2^3 + l_2 \end{bmatrix}$$

$$Q_C = \begin{bmatrix} -r & 0 & 0 & 0 & 0 & 0 \\ 0 & -l_2 & 0 & 0 & 0 & 0 \\ 0 & 0 & -r & 0 & 0 & 0 \\ 0 & 0 & 0 & -l_2 & 0 & 0 \\ 0 & 0 & 0 & 0 & -r & 0 \\ 0 & 0 & 0 & 0 & 0 & -l_2 \end{bmatrix}$$

We can see that the Q_C matrix is invertible as long as r and l_2 are not zero. So the inverse kinematics is

$$\dot{q}_C = Q_C^{-1} P_C \begin{bmatrix} \dot{X}_b \\ \dot{\eta} \end{bmatrix} \quad (18)$$

The task space X can be divided into one part $\dot{X}_b = [\dot{x}_b \ \dot{y}_b \ \dot{\psi}_b]^T$ dealing with the trajectory tracking and the other part $\eta = [\theta_{11} \ \theta_{21} \ \theta_{31}]^T$ dealing with the posture of the legs. To solve the redundancy, we could control these two parts separately. For posture control, we applied an error space control law to maintain the desired arrangement of the legs:

$$\dot{\eta}_d = K_\eta (\eta_r - \eta) + \dot{\eta}_r \quad (19)$$

For path following task, we use a simple control law

$$\dot{\xi}_d = K_\xi (\xi_r - \xi) + \dot{\xi}_r \quad (20)$$

where ξ_r is the reference path that the robot have to follow and ξ is the sensed position of the robot, both in Cartesian space. With proper selection of K_η and K_ξ , the convergence of error $\eta_r - \eta$ and $\xi_r - \xi$ could be guaranteed. Note that $\dot{\xi}_d$ is expressed in inertial frame, in order to use the inverse kinematic model Eq. (19) we transform it into body frame by

$${}^B R_F = \begin{bmatrix} \cos \psi & \sin \psi & 0 \\ -\sin \psi & \cos \psi & 0 \\ 0 & 0 & 1 \end{bmatrix}$$

To find the corresponding wheel steering and driving joint rates \dot{q}_C , we could use

$$\dot{q}_C = Q_C^{-1} P_C \begin{bmatrix} \dot{X}_{db} \\ \dot{\eta}_d \end{bmatrix} \quad (21)$$

where \dot{X}_{db} is the desired base motion expressed in body frame

$$\dot{X}_{db} = {}^B R_F \dot{\xi}_d \quad (22)$$

At last, nine PI velocity controllers will be used to control all nine joint rates independently. (Note that here we actually use redundant actuation to improve the stiffness and dynamic property of the system) The overall control scheme is shown in Fig. 4.

Control Scheme II

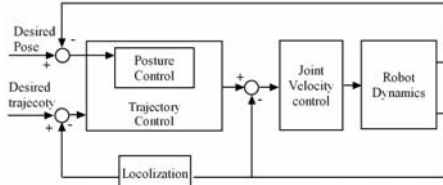


FIGURE 5: DIAGRAM OF KINEMATIC CONTROL SCHEME II

The first controller needs designer's intuition to find the proper velocities for a subset of all joints. It depends on the physical design and is not general enough. In the second control scheme, we will discuss a more general method that could be potentially used for other AWRs. As there are two control tasks and the path following part has the first priority, we could use pseudoinverse and potential function techniques to resolve redundancy. Recall that the kinematic equation Eq. 18 is:

$$P_A \dot{X}_b = Q_A \dot{q}_A$$

The desired base motion \dot{X}_{db} is found using the same way in control scheme I. Since Q_A is always full rank and has more columns than rows, to resolve the redundant actuation, we use the following control scheme

$$\dot{q}_A = Q_A^\# P_A \dot{X}_{db} + [I - Q_A^\# Q_A] Z \quad (23)$$

where $Q_A^\# = Q_A^T (Q_A Q_A^T)^{-1}$ is the pseudo inverse of Q_A , and $Z = -\nabla V$ is a potential function that drives the posture error to zero, where

$$V = K [(\theta_{11} - \theta_{11}^d)^2 + (\theta_{21} - \theta_{21}^d)^2 + (\theta_{31} - \theta_{31}^d)^2] \quad (24)$$

The particular part of Eq. (25) controls the robot to achieve the primary task, path following, by mapping the desired base motion to joint space. The homogeneous part of Eq. (25) is designed to achieve the secondary task, leg position regulation. When $\dot{X}_{db} = 0$, Eq. 26 guarantees monotonous decrease of the potential function. When the desired joint rates of all 9 joints are obtained, we use 9 independent PI controllers to control each joint. The control diagram is shown in Fig. 5.

SIMULATION RESULT

The simulation is done in MATLAB. The dynamic model was constructed by importing CAD model into SimMechanics then adding velocity constraints between wheels and ground. Therefore the model is a perfect model. The robot parameters used in the simulations are shown in Table 2

TABLE 2: SIMULATION PARAMETERS OF THE ROAMER

l_0	0.2m	m_{body}	7kg
l_1	0.3m	m_{leg}	0.237kg
l_2	0.05m	m_{wheel}	0.206kg
r	0.05m		

In both simulations, the path following task is to drive the robot to a circular path with center at (0.5m, 0m) and radius 1m. The reconfiguration task is to move all the legs in a sinusoidal

motion $\theta_{il} = 2\pi/3\sin(t)$. This sinusoidal motion will effectively change the configuration of the wheels (or supporting polygon) between a large triangle with approximate side length 0.87m and a small triangle with approximate side length 0.43m.

Control Scheme I

The control performance of control scheme I is shown in Fig. 6 and Fig. 7. We could see clearly that the robot could follow the desired path nicely and small leg position error shown in Fig. 7 shows that the configuration of the robot can change smoothly during whole locomotion period. This result indicates the capability of the ROAMeR for various applications that require the base to change its shape to avoid obstacles and improve stability. The redundancy in the system has been resolved.

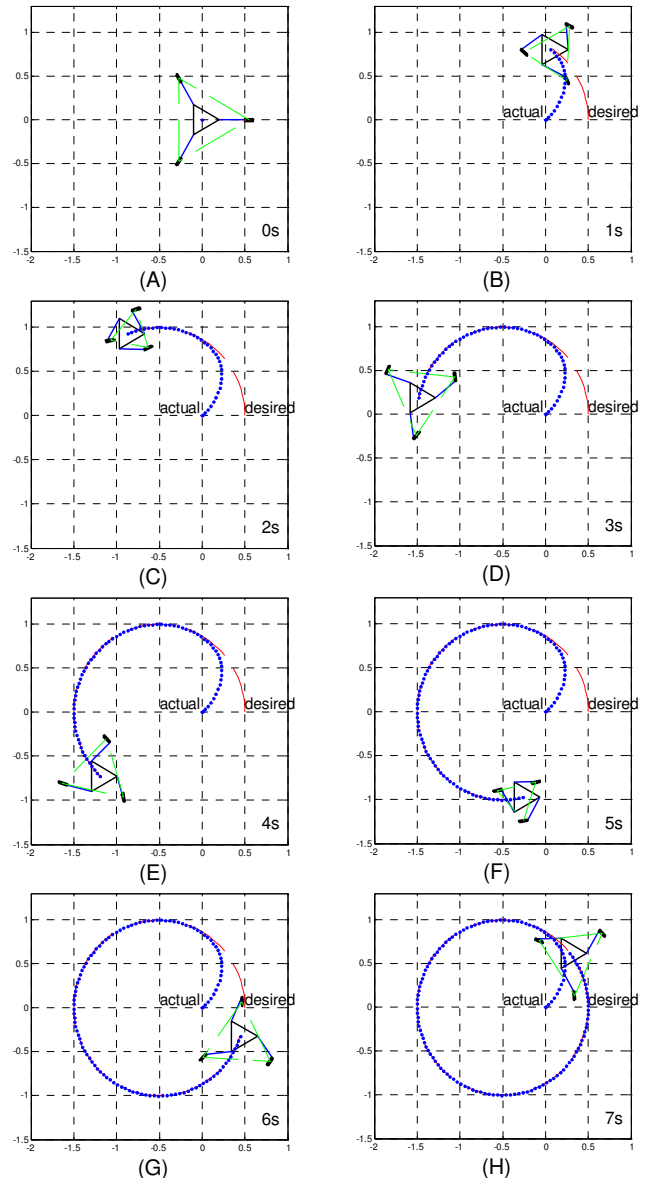


FIGURE 6: SIMULATION SCREEN SHOTS OF CONTROL SCHEME I, PATH FOLLOWING, (A) ~ (H): 0 ~7S

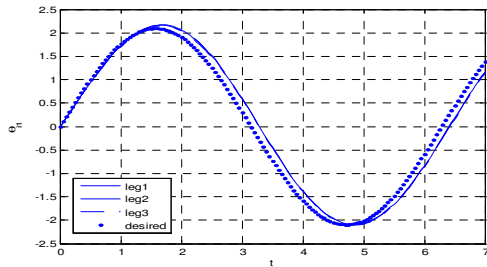


FIGURE 7: SIMULATION RESULT OF CONTROL SCHEME I, LEG POSITION REGULATION PERFORMANCE

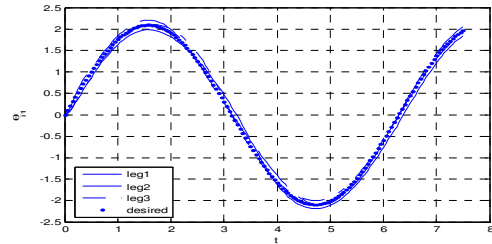


FIGURE 9: SIMULATION RESULT OF CONTROL SCHEME I, LEG POSITION REGULATION PERFORMANCE

Control Scheme II

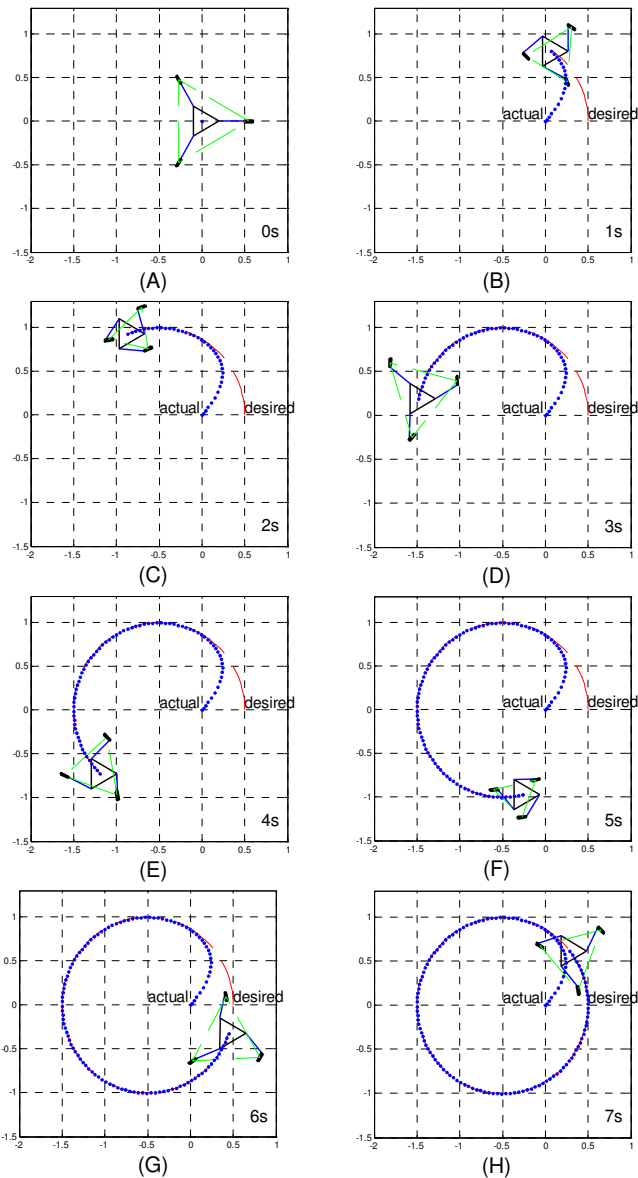


FIGURE 8: SIMULATION SCREEN SHOTS OF CONTROL SCHEME II, PATH FOLLOWING, (A) ~ (H): 0 ~ 7S

The control performance of control scheme II is shown in Fig. 8 and Fig. 9. The robot again could follow the desired path nicely. The leg position error shown in Fig. 9 is small and slightly different from the result of control scheme I. We also notice that when the robot performing locomotion and reconfiguration tasks, it can be observed that the three casters acts like three mobile manipulators transporting a large payload, the reconfiguration process is effectively formation change of the three 'caster robots'.

PROTOTYPING

Two physical prototypes have been built. The first one is a simple prototype of the ROAMeR concept with RC servos as joint actuators, as shown in Fig. 10, an open loop controller running in MATLAB sends velocity command through serial port to Lynxmotion servo controller board which controls the servos. It shows that both path following and reconfiguration could be possibly achieved in real world.

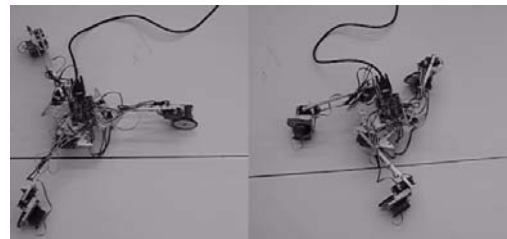


FIGURE 10: SERVO ACTUATED PROTOTYPE I IN MOTION

The construction of a more rugged second prototype, whose CAD drawing and physical prototype is shown in Figure 11, is currently nearing completion. In addition to machined structural components, the system is energy independent and possesses more reliable actuation and sensing (dc motors/encoders) controlled within an onboard PC104 platform running the xPCTarget real-time operating system.



FIGURE 11: PROTOTYPE II (A) CAD DRAWING AND (B) PHYSICAL MODEL

CONCLUSIONS

Articulated wheeled robots have considerable benefits by virtue of their reconfigurability and redundancy – but these need to be unlocked by careful modeling, analysis and control. In this paper, we examined a twist-based kinematic modeling method for articulated wheeled robots to help systematize the modeling of such complicated systems for subsequent analysis and control. This framework was deployed and tested in the case-study of a planar omnidirectional mobile robot capable of such reconfiguration. Two kinematic control schemes are developed and the results are studied to solve the issues of maintaining kinematic consistency of the constraints and resolving the redundancies inherent in such articulated wheeled robots. Planned future work includes real-time kinematic experiments on the second physical prototype, developing localization and dynamic control algorithms, reconfiguration planning and expanding our modeling frame work and control scheme into 3D AWRs moving on uneven terrain.

ACKNOWLEDGMENTS

We gratefully acknowledge the support from National Science Foundation CAREER Award (IIS-0347653) for this research effort.

REFERENCES

- [1] Hacot, H., Dubowsky, S., and Bidaud, P., 1998, "Analysis and Simulation of a Rocker-Bogie Exploration Rover," Twelfth CISM-IFTOMM Symposium (RoManSy 98), Paris, France.
- [2] Siegwart, R., Lamon, P., Estier, T., Lauria, M., and Piguat, R., 2002, "Innovative design for wheeled locomotion in rough terrain," *Robotics and Autonomous Systems*, 40, pp. 151-162.
- [3] Halme, A., Leppanen, I., Soumela, J., Ylonen, S., and Kettunen, I., 2003, "WorkPartner: interactive human-like service robot for outdoor applications," *International Journal of Robotics Research*, 22(7-8), pp. 627-640.
- [4] Wada, M., and Asada, H. H., 1999, "Design and control of a variable footprint mechanism for holonomic omnidirectional vehicles and its application to wheelchairs," *IEEE Transactions on Robotics and Automation*, 15(6), pp. 978-989.
- [5] Iagnemma, K., Rzepniewski, A., and Dubowsky, S., 2003, "Control of robotic vehicles with actively articulated suspensions in rough terrain," *Autonomous Robots*, 14(1), pp. 5-16.
- [6] Wilcox, B. H., Litwin, T. E., Biesiadecki, J. J., Matthews, J. B., Heverly, M. C., Morrison, J. C., Townsend, J. A., Ahmad, N. M., Sirota, A. R., and Cooper, B. K., 2007, "ATHLETE: A cargo handling and manipulation robot for the moon," *Journal of Field Robotics*, 24(5), pp. 421-434.
- [7] Sreenivasan, S. V., and Waldron, K. J., 1996, "Displacement analysis of an actively articulated wheeled vehicle configuration with extensions to motion planning on uneven terrain," *Journal of Mechanical Design, Transactions of the ASME*, 118(2), pp. 312-317.
- [8] Grand, C., Benamar, F., Plumet, F., and Bidaud, P., 2004, "Stability and traction optimization of a reconfigurable wheel-legged robot," *International Journal of Robotics Research*, 23(10-11), pp. 1041-1058.
- [9] Muir, P. F., and Neuman, C. P., 1987, "Kinematic modeling of wheeled mobile robots," *Journal of Robotic Systems*, 4(2), pp. 281-340.
- [10] Campion, G., Bastin, G., and D'Andrea-Novell, B., 1996, "Structural properties and classification of kinematic and dynamic models of wheeled mobile robots," *IEEE Transactions on Robotics and Automation*, 12(1), pp. 47-62.
- [11] Yi, B.-J., and Kim, W. K., 2002, "The kinematics for redundantly actuated omnidirectional mobile robots," *Journal of Robotic Systems*, 19(6), pp. 255-267.
- [12] Tarokh, M., and McDermott, G. J., 2005, "Kinematics modeling and analyses of articulated rovers," *IEEE Transactions on Robotics*, 21(4), pp. 539-553.
- [13] Choi, B. J., and Sreenivasan, S. V., 2001, "Partial Contact Force Controllability in Active Wheeled Vehicles," *Journal of Mechanical Design*, 123(2), pp. 169-175.
- [14] Song, J.-B., and Byun, K.-S., 2004, "Design and control of a four-wheeled omnidirectional mobile robot with steerable omnidirectional wheels," *Journal of Robotic Systems*, 21(4), pp. 193-208.
- [15] Holmberg, R., and Khatib, O., 2000, "Development and control of a holonomic mobile robot for mobile manipulation tasks," *International Journal of Robotics Research*, 19(11), pp. 1066-1074.